Electronic Supplementary Material (ESI) for Nanoscale.


# Supporting Information

# Two-dimensional $MN_4$ Materials as Effective Multifunctional Electrocatalyst for Oxygen Reduction, Oxygen Evolution, and Hydrogen Evolution Reactions

**Xian Zhang[+1], Zhifen Luo[+1], Jiayi Fan[2], Tengfei Cao[1], Junqin Shi [1], Xiaoli Fan [1*]**

[1] State Key Laboratory of Solidification Processing, Center for Advanced Lubrication and Seal Materials, School of Material Science and Engineering, Northwestern Polytechnical University, 127 YouYi Western Road, Xi'an, Shaanxi 710072, China

[2] School of Material Science and Engineering, Northwestern Polytechnical University, 127 YouYi Western Road, Xi'an, Shaanxi 710072, China

[+] Xian Zhang and Zhifen Luo contributed equally to this work

* xlfan@nwpu.edu.cn

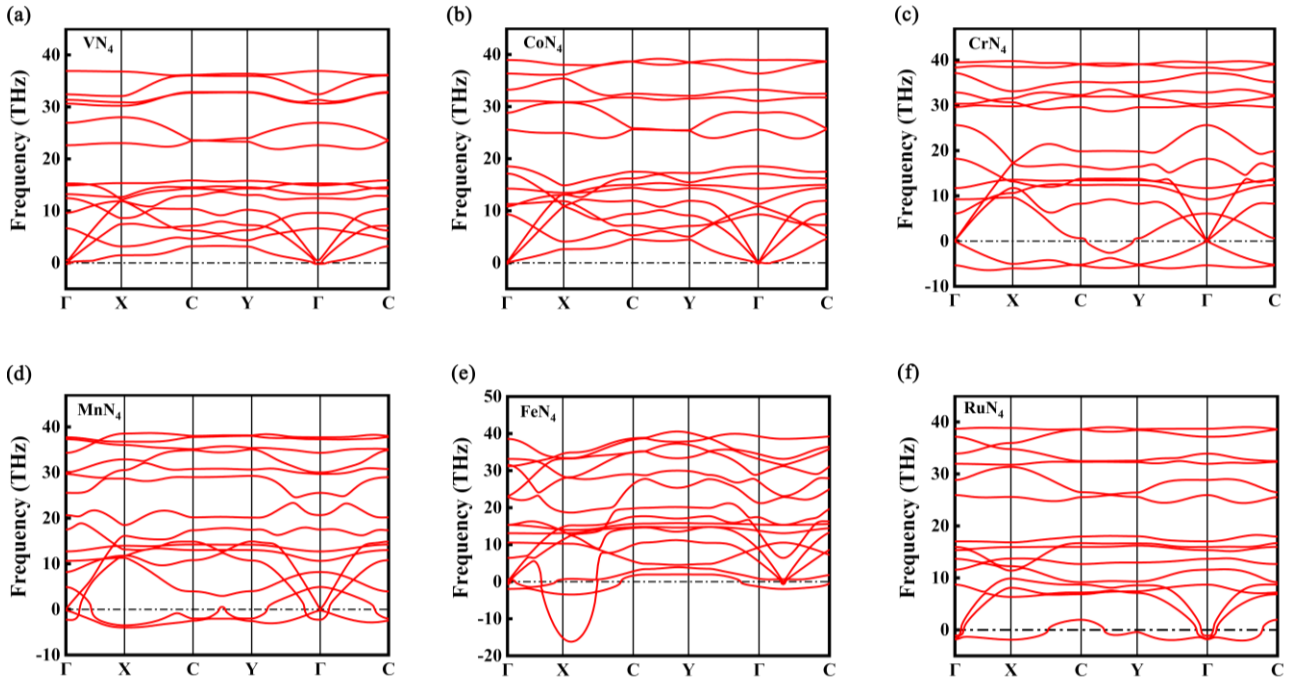


**Figure S1.** Phonon dispersion of (a) $VN_4$, (b) $CoN_4$, (c) $CrN_4$, (d) $MnN_4$, (e) $FeN_4$, (f) $RuN_4$ monolayers.

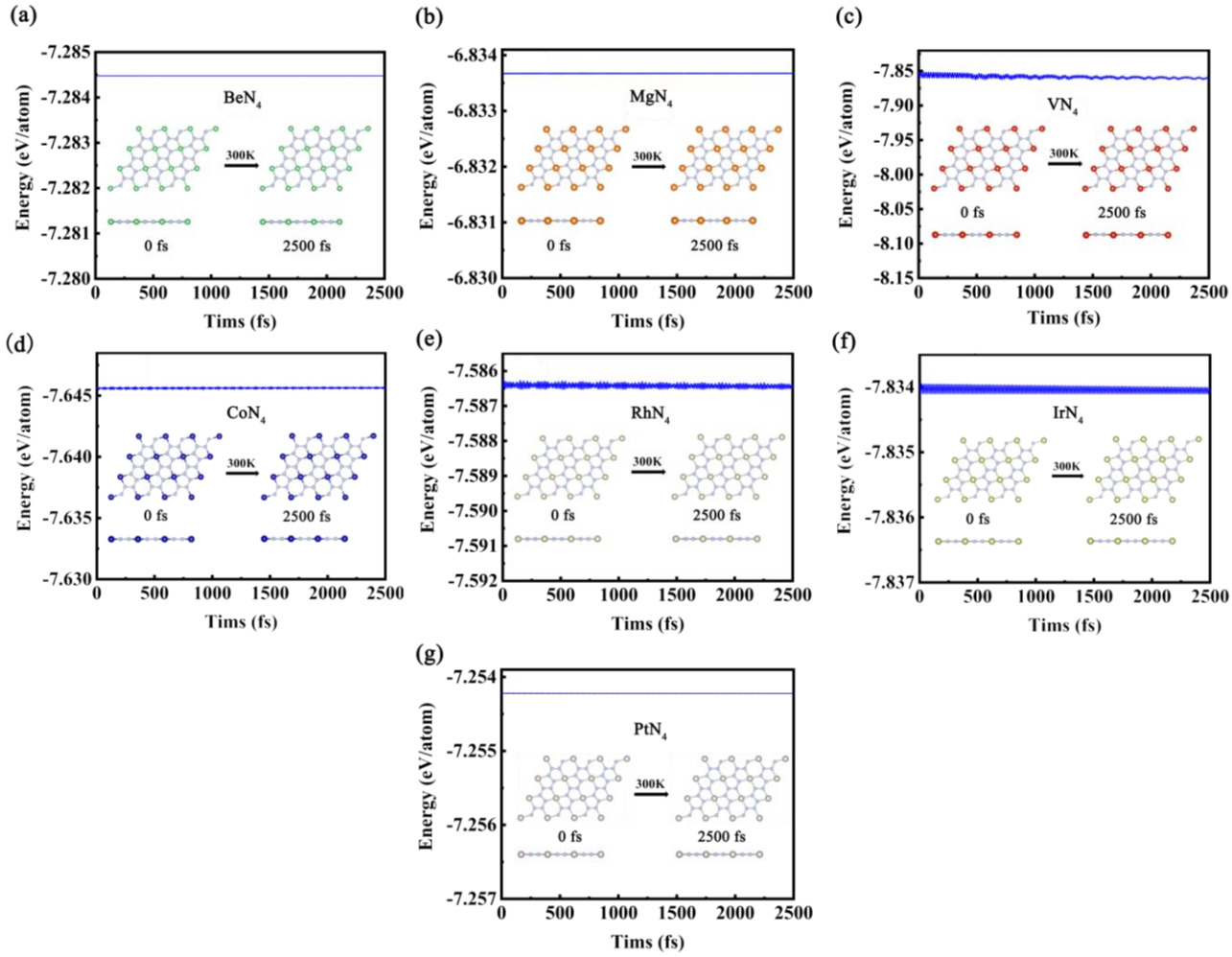


**Figure S2.** Evolution of the total energy for (a) $BeN_4$, (b) $MgN_4$, (c) $VN_4$, (d) $CoN_4$, (e) $RhN_4$ (f) $IrN_4$, (g) $PtN_4$ monolayers during the *ab-inito* molecular dynamics (AIMD) simulations for 2500 fs at 300 K. The inset diagrams show the side and top views of the atomic structures at the starting and end of the AIMD simulation.

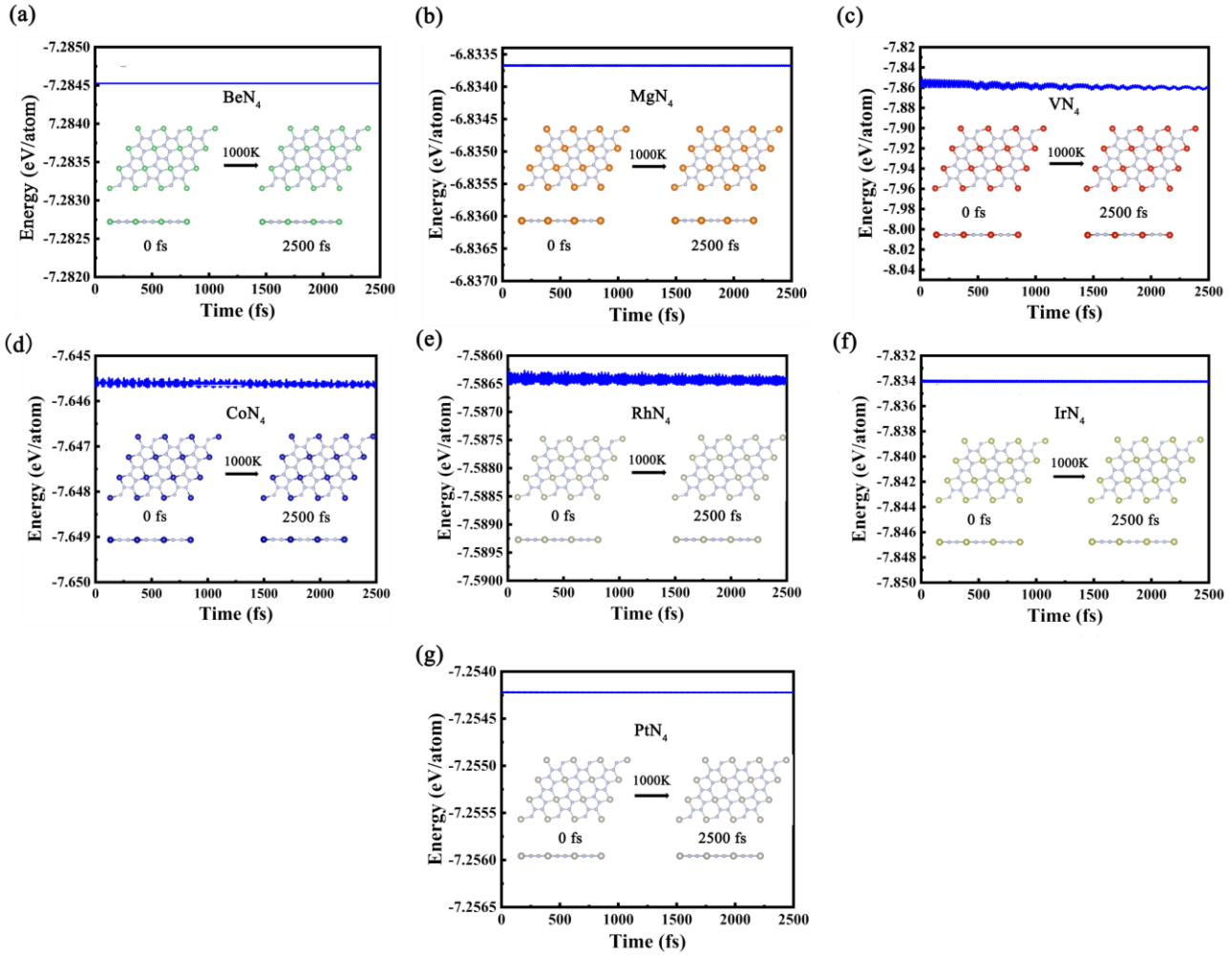


**Figure S3.** Evolution of the total energy for (a) $BeN_4$, (b) $MgN_4$, (c) $VN_4$, (d) $CoN_4$, (e) $RhN_4$ (f) $IrN_4$, (g) $PtN_4$ monolayers during the *ab-inito* molecular dynamics (AIMD) simulations for 2500 fs at 1000 K. The inset diagrams show the side and top views of the atomic structures at the starting and end of the AIMD simulation.

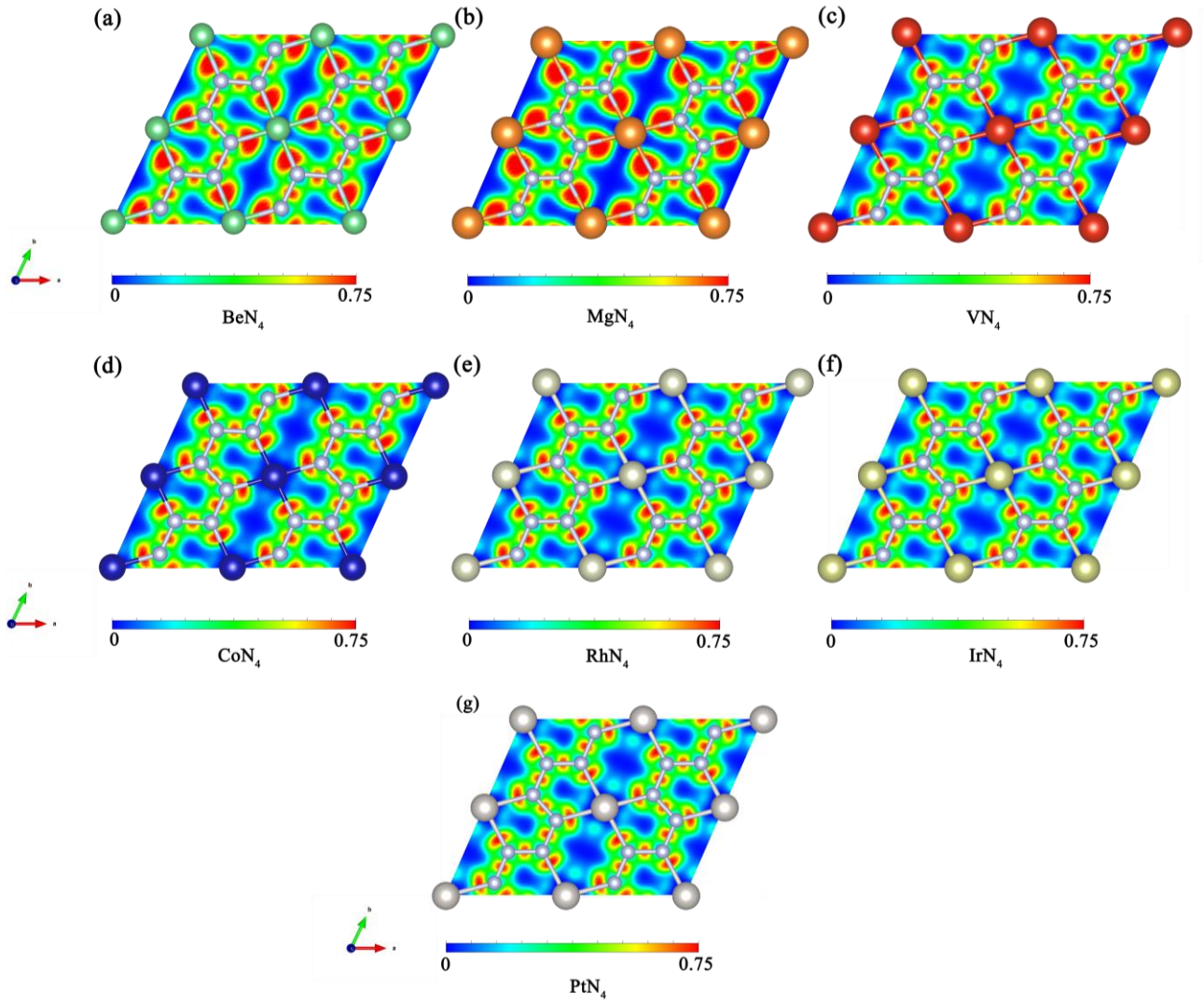


**Figure S4.** The electron localization function (ELF) on the atomic plane of (a) $BeN_4$, (b) $MgN_4$, (c) $VN_4$, (d) $CoN_4$, (e) $RhN_4$, (f) $IrN_4$, (g) $PtN_4$ monolayers.

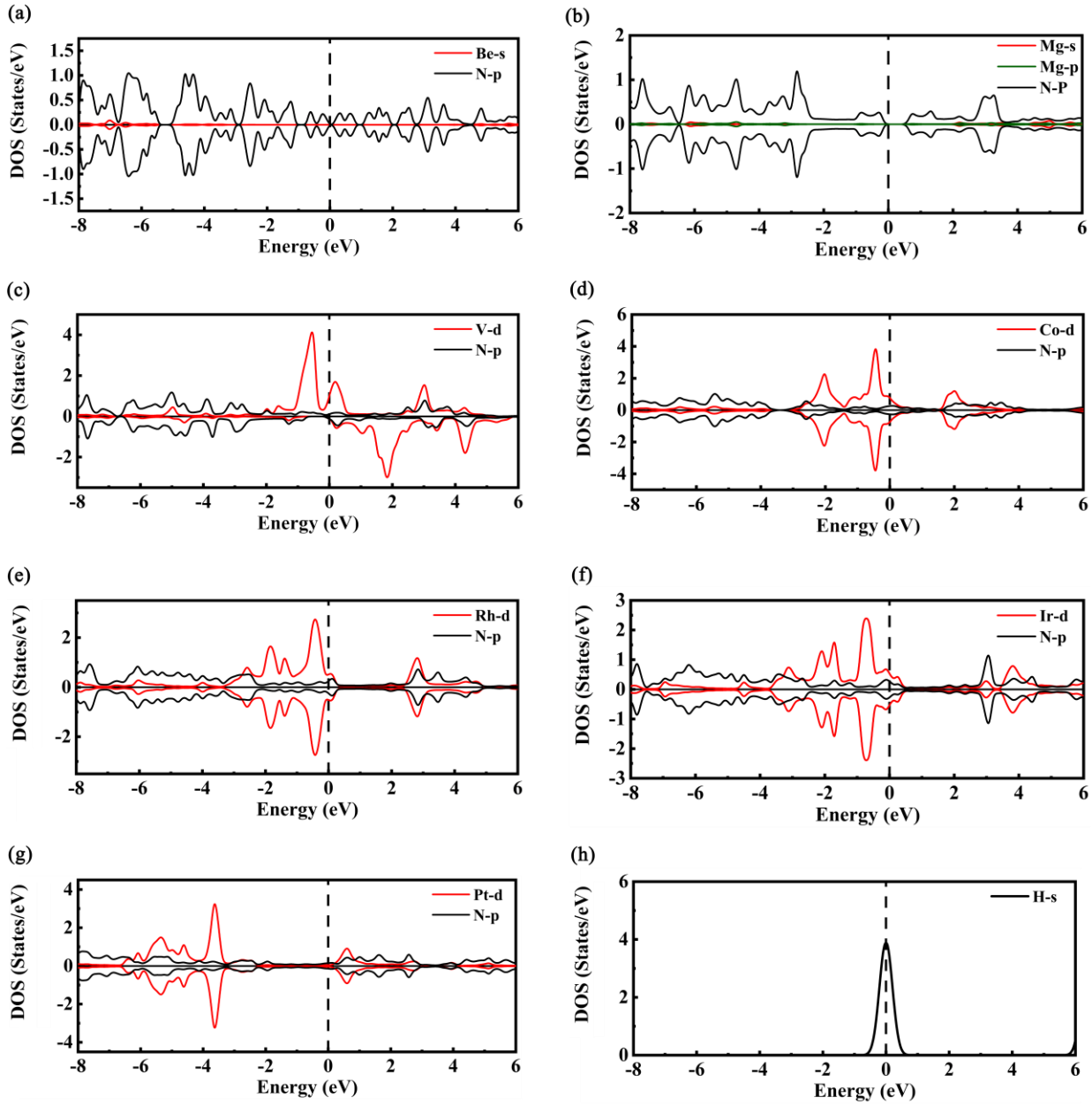


**Figure S5.** The projected density of states (DOS) of M and N atoms in $MN_4$ (M = Be, Mg, V, Co, Rh, Ir, Pt) monolayer, (a) $BeN_4$, (b) $MgN_4$, (c) $VN_4$, (d) $CoN_4$, (e) $RhN_4$, (f) $IrN_4$, (g) $PtN_4$, and the DOS of (h) H atom.

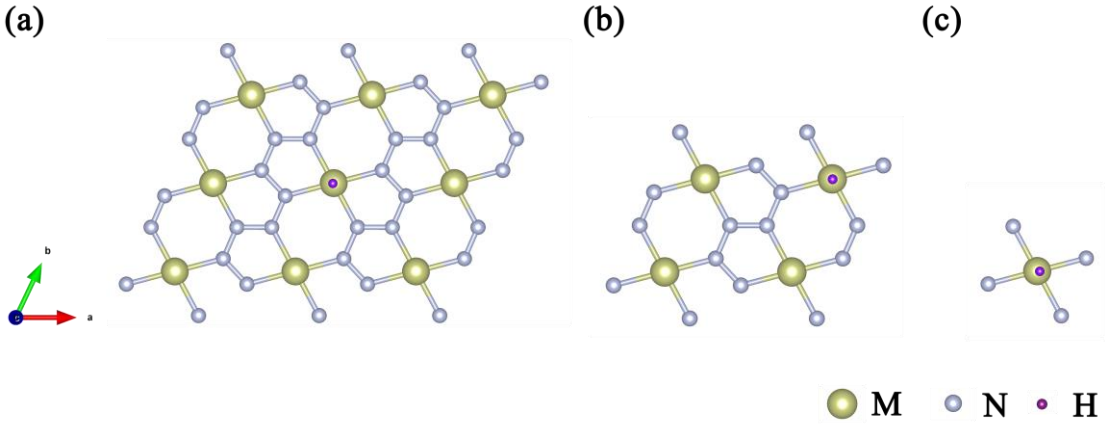


**Figure S6.** Schematic diagram showing the supercells of $MN_4$ monolayer used for modeling (a) 11%, (b) 25%, and (c) 100% M atoms participating in reaction. Yellow, silver, and purple balls represent the M, N, and H atoms, respectively.

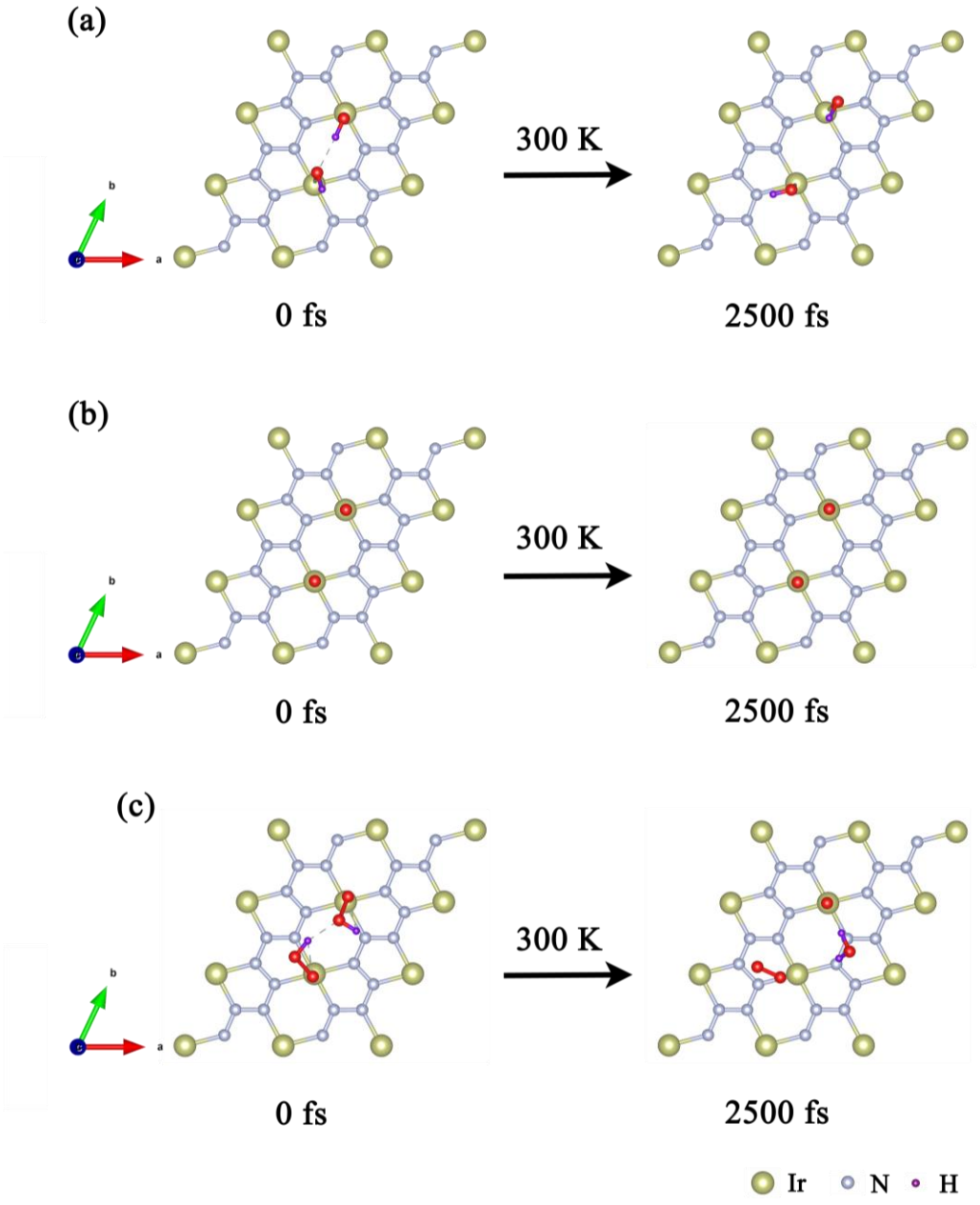


**Figure S7.** The atomic structures at the starting and end of the *ab-initio* molecular dynamics (AIMD) simulations for 2500 fs at 300 K for two (a) OH*, (b) O*, and (c) OOH* species absorb on the two nearest neighboring Ir atoms on $IrN_4$ monolayer.

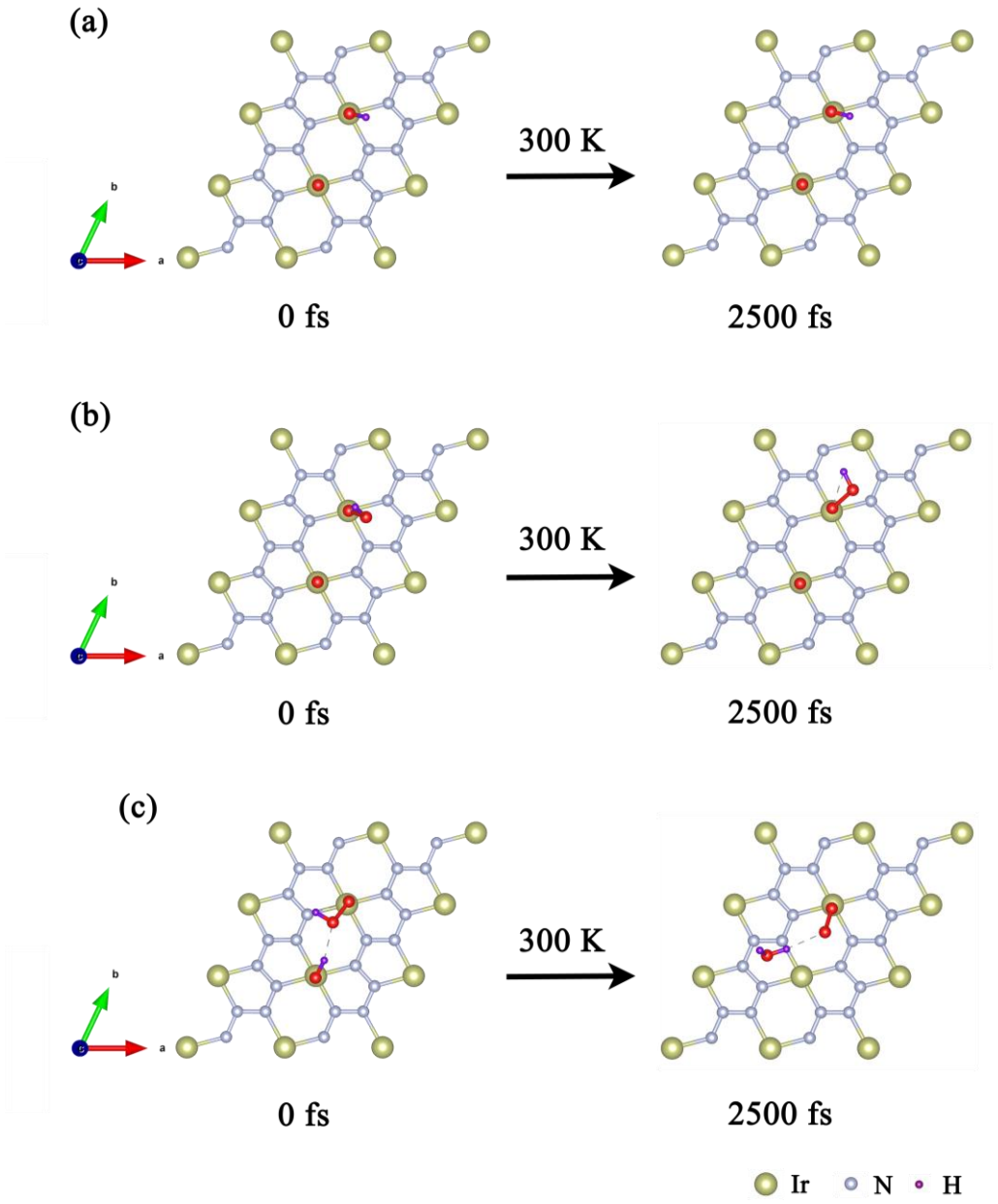


**Figure S8.** The atomic structures at the starting and end of the *ab-initio* molecular dynamics (AIMD) simulations for 2500 fs at 300 K for (d) OH* and O*, (e) O* and OOH*, (f) OH* and OOH* absorbing on the two nearest neighboring Ir atoms on $IrN_4$ monolayer.

**Table S1.** The calculated energies (E) of $H_2O$ and $H_2$ molecules in gas phase, the zero-point energy corrections (ZPE) and entropy contributions (TS) of $H_2O$, $H_2$ at 298.15 K.

| Species | E (eV) | ZPE (eV) | TS (eV) |
|---|---|---|---|
| $H_2O$ | -14.21 | 0.55 | 0.56 |
| $H_2$ | -6.72 | 0.27 | 0.35 |

**Table S2** The zero-point energy corrections (ZPE) and entropy contributions (TS) of H* OH*, O*, and OOH* on $MN_4$ (M = Be, Mg, V, Co, Rh, Ir, Pt) monolayers at 298.15K with 11% M atoms participating in reaction.

| $MN_4$ | Species | ZPE (eV) | TS (eV) |
|---|---|---|---|
| $BeN_4$ | H* | 0.18 | 0.01 |
| | OH* | 0.40 | 0.11 |
| | O* | 0.11 | 0.11 |
| | OOH* | 0.54 | 0.21 |
| $MgN_4$ | H* | 0.24 | 0.02 |
| | OH* | 0.39 | 0.16 |
| | O* | 0.09 | 0.12 |
| | OOH* | 0.53 | 0.18 |
| $VN_4$ | H* | 0.18 | 0.02 |
| $CoN_4$ | H* | 0.20 | 0.01 |
| | OH* | 0.40 | 0.12 |
| | O* | 0.10 | 0.08 |
| | OOH* | 0.51 | 0.14 |
| $RhN_4$ | H* | 0.21 | 0.01 |
| | OH* | 0.40 | 0.13 |
| | O* | 0.09 | 0.08 |
| | OOH* | 0.54 | 0.21 |
| $IrN_4$ | H* | 0.22 | 0.01 |
| | OH* | 0.41 | 0.13 |
| | O* | 0.10 | 0.08 |
| | OOH* | 0.53 | 0.20 |
| $PtN_4$ | H* | 0.24 | 0.01 |
| | OH* | 0.43 | 0.13 |
| | O* | 0.12 | 0.12 |
| | OOH* | 0.63 | 0.30 |

**Table S3** The zero-point energy corrections (ZPE) and entropy contributions (TS) of H* OH*, O*, and OOH* on $MN_4$ (M = Be, Mg, V, Co, Rh, Ir, Pt) monolayers at 298.15K with 25% M atoms participating in reaction.

| $MN_4$ | Species | ZPE (eV) | TS (eV) |
|---|---|---|---|
| $BeN_4$ | H* | 0.18 | 0.01 |
| | OH* | 0.40 | 0.11 |
| | O* | 0.09 | 0.08 |
| | OOH* | 0.54 | 0.21 |
| $MgN_4$ | H* | 0.21 | 0.02 |
| | OH* | 0.39 | 0.17 |
| | O* | 0.09 | 0.12 |
| | OOH* | 0.53 | 0.25 |
| $VN_4$ | H* | 0.18 | 0.02 |
| $CoN_4$ | H* | 0.20 | 0.01 |
| | OH* | 0.40 | 0.12 |
| | O* | 0.10 | 0.08 |
| | OOH* | 0.53 | 0.19 |
| $RhN_4$ | H* | 0.21 | 0.01 |
| | OH* | 0.40 | 0.13 |
| | O* | 0.09 | 0.08 |
| | OOH* | 0.54 | 0.21 |
| $IrN_4$ | H* | 0.22 | 0.01 |
| | OH* | 0.41 | 0.13 |
| | O* | 0.10 | 0.08 |
| | OOH* | 0.53 | 0.20 |
| $PtN_4$ | H* | 0.24 | 0.01 |
| | OH* | 0.38 | 0.18 |
| | O* | 0.09 | 0.11 |
| | OOH* | 0.52 | 0.31 |

**Table S4** The zero-point energy corrections (ZPE) and entropy contributions (TS) of H* OH*, O*, and OOH* on $MN_4$ (M = Be, Mg, V, Co, Rh, Ir, Pt) monolayers at 298.15K with 100% M atoms participating in reaction.

| $MN_4$ | Species | ZPE (eV) | TS (eV) |
|---|---|---|---|
| $BeN_4$ | H* | 0.18 | 0.01 |
| | OH* | 0.38 | 0.08 |
| | O* | 0.09 | 0.08 |
| | OOH* | 0.46 | 0.16 |
| $MgN_4$ | H* | 0.19 | 0.01 |
| | OH* | 0.30 | 0.04 |
| | O* | 0.23 | 0.24 |
| | OOH* | 0.53 | 0.24 |
| $VN_4$ | H* | 0.19 | 0.02 |
| $CoN_4$ | H* | 0.20 | 0.01 |
| | OH* | 0.40 | 0.11 |
| | O* | 0.10 | 0.08 |
| | OOH* | 0.53 | 0.18 |
| $RhN_4$ | H* | 0.20 | 0.02 |
| | OH* | 0.38 | 0.10 |
| | O* | 0.09 | 0.08 |
| | OOH* | 0.54 | 0.19 |
| $IrN_4$ | H* | 0.21 | 0.02 |
| | OH* | 0.41 | 0.13 |
| | O* | 0.10 | 0.08 |
| | OOH* | 0.52 | 0.19 |
| $PtN_4$ | H* | 0.24 | 0.01 |
| | OH* | 0.38 | 0.17 |
| | O* | 0.08 | 0.14 |
| | OOH* | 0.50 | 0.19 |

**Table S5.** The lattice constants, bond lengths, dynamical stability, cohesive energies ($E_{coh}$), formation energies ($E_f$) and dissolution potential ($U_{dis}$) of $MN_4$ (M = Be, Mg, V, Cr, Mn, Fe, Co, Ru, Rh, Ir, Pt) monolayers.

| $MN_4$ | Lattice constant | | | Bond length | | | Dynamical stability | $E_{coh}$ (eV) | $E_f$ (eV) | $U_{dis}$ (V) |
|---|---|---|---|---|---|---|---|---|---|---|
| | a (Å) | b (Å) | γ (°) | TM-N | $N_1$-$N_2$ | $N_2$-$N_3$ | | | | |
| **$BeN_4$** | 4.27 | 3.66 | 64.59 | 1.75 | 1.34 | 1.34 | √ | 4.82 | 0.60 | 0.04 |
| **$MgN_4$** | 4.83 | 3.86 | 66.45 | 2.06 | 1.35 | 1.35 | √ | 4.36 | 6.30 | 0.37 |
| **$VN_4$** | 4.82 | 3.79 | 66.85 | 2.01 | 1.35 | 1.36 | √ | 4.86 | 1.80 | 0.42 |
| **$CrN_4$** | 4.76 | 3.78 | 66.62 | 1.98 | 1.34 | 1.36 | × | | | |
| **$MnN_4$** | 4.60 | 3.75 | 65.96 | 1.89 | 1.35 | 1.38 | × | | | |
| **$FeN_4$** | 4.51 | 3.72 | 65.62 | 1.85 | 1.34 | 1.37 | × | | | |
| **$CoN_4$** | 4.44 | 3.70 | 65.43 | 1.82 | 1.34 | 1.36 | √ | 4.87 | 1.85 | 0.55 |
| **$RuN_4$** | 4.72 | 3.77 | 66.51 | 1.97 | 1.33 | 1.36 | × | | | |
| **$RhN_4$** | 4.73 | 3.78 | 66.47 | 1.98 | 1.33 | 1.33 | √ | 4.89 | 2.25 | 1.09 |
| **$IrN_4$** | 4.72 | 3.77 | 66.51 | 1.96 | 1.34 | 1.36 | √ | 4.90 | 2.55 | 1.27 |
| **$PtN_4$** | 4.73 | 3.79 | 66.37 | 1.98 | 1.33 | 1.36 | √ | 4.49 | 2.65 | 0.81 |

**Table S6.** Gibbs free energy change of hydrogen adsorption ($\Delta G_{H^*}$**)** at M atom on $MN_4$ (M = Be, Mg, V, Co, Rh, Ir, Pt) monolayers with 11%, 25%, and 100% M atoms participating in reaction.

| System | $\Delta G_{H^*}$ (eV) | | |
|---|---|---|---|
| | **11%** | **25%** | **100%** |
| **$BeN_4$** | 1.16 | 1.05 | 1.21 |
| **$MgN_4$** | 0.69 | 0.83 | 1.29 |
| **$VN_4$** | 0.06 | -0.01 | 0.14 |
| **$CoN_4$** | 0.37 | 0.38 | 0.47 |
| **$RhN_4$** | 0.14 | 0.14 | 0.40 |
| **$IrN_4$** | -0.01 | -0.01 | 0.11 |
| **$PtN_4$** | 1.04 | 0.97 | 1.63 |

**Table S7.** Gibbs free energy change of intermediate OH adsorption ($\Delta G_{OH*}$), O adsorption ($\Delta G_{O*}$), OOH adsorption ($\Delta G_{OOH*}$), the four reaction steps ($\Delta G_1 \sim \Delta G_4$), and the overpotentials ($\eta$) of oxygen evolution reaction (OER) and oxygen reduction reaction (ORR) on $MN_4$ (M = Be, Mg, Co, Rh, Ir, Pt) monolayers with 11% M atoms participating in reaction. The results of OER and ORR are presented in red and blue color, respectively.

| System | $\Delta G_{OH*}$ (eV) | $\Delta G_{O*}$ (eV) | $\Delta G_{OOH*}$ (eV) | $\Delta G_1$ (eV) | $\Delta G_2$ (eV) | $\Delta G_3$ (eV) | $\Delta G_4$ (eV) | $\eta$ (V) |
|---|---|---|---|---|---|---|---|---|
| **$BeN_4$** | 0.06 | 2.64 | 3.36 | 0.06 | 2.57 | 0.72 | 1.56 | 1.34 |
| | | | | -1.56 | -0.72 | -2.57 | -0.06 | 1.17 |
| **$MgN_4$** | -0.37 | 1.90 | 2.62 | -0.37 | 2.27 | 0.72 | 2.30 | 1.07 |
| | | | | -2.30 | -0.72 | -2.27 | 0.37 | 1.60 |
| **$CoN_4$** | 0.96 | 2.45 | 3.95 | 0.96 | 1.49 | 1.50 | 0.97 | 0.26 |
| | | | | -0.97 | -1.50 | -1.49 | -0.96 | 0.26 |
| **$RhN_4$** | 0.99 | 3.14 | 4.16 | 0.99 | 2.15 | 1.02 | 0.76 | 0.92 |
| | | | | -0.76 | -1.02 | -2.15 | -0.99 | 0.47 |
| **$IrN_4$** | 0.82 | 2.40 | 3.75 | 0.82 | 1.58 | 1.35 | 1.17 | 0.35 |
| | | | | -1.17 | -1.35 | -1.58 | -0.82 | 0.41 |
| **$PtN_4$** | 1.58 | 3.74 | 4.44 | 1.58 | 2.16 | 0.70 | 0.48 | 0.93 |
| | | | | -0.48 | -0.70 | -2.16 | -1.58 | 0.75 |

**Table S8.** Gibbs free energy changes of intermediate OH adsorption ($\Delta G_{OH*}$), O adsorption ($\Delta G_{O*}$), OOH adsorption ($\Delta G_{OOH*}$), the four reaction steps ($\Delta G_1 \sim \Delta G_4$), and the overpotentials ($\eta$) of oxygen evolution reaction (OER) and oxygen reduction reaction (ORR) on $MN_4$ (M = Be, Mg, Co, Rh, Ir, Pt) monolayers with 25% M atoms participating in reaction. The results of OER and ORR are presented in red and blue color, respectively.

| System | $\Delta G_{OH*}$ (eV) | $\Delta G_{O*}$ (eV) | $\Delta G_{OOH*}$ (eV) | $\Delta G_1$ (eV) | $\Delta G_2$ (eV) | $\Delta G_3$ (eV) | $\Delta G_4$ (eV) | $\eta$ (V) |
|---|---|---|---|---|---|---|---|---|
| **$BeN_4$** | -0.01 | 2.58 | 3.39 | -0.01 | 2.59 | 0.81 | 1.53 | 1.36 |
| | | | | -1.53 | -0.81 | -2.59 | 0.01 | 1.24 |
| **$MgN_4$** | -0.24 | 2.13 | 3.07 | -0.24 | 2.37 | 0.94 | 1.85 | 1.14 |
| | | | | -1.85 | -0.94 | -2.37 | 0.24 | 1.47 |
| **$CoN_4$** | 1.01 | 2.58 | 3.92 | 1.01 | 1.57 | 1.34 | 1.00 | 0.34 |
| | | | | -1.00 | -1.34 | -1.57 | -1.01 | 0.22 |
| **$RhN_4$** | 1.20 | 3.11 | 4.12 | 1.20 | 1.91 | 1.01 | 0.80 | 0.68 |
| | | | | -0.80 | -1.01 | -1.91 | -1.20 | 0.43 |
| **$IrN_4$** | 0.91 | 2.47 | 3.84 | 0.91 | 1.56 | 1.38 | 1.08 | 0.33 |
| | | | | -1.08 | -1.38 | -1.56 | -0.91 | 0.32 |
| **$PtN_4$** | 1.32 | 3.50 | 4.05 | 1.32 | 2.18 | 0.55 | 0.87 | 0.95 |
| | | | | -0.87 | -0.55 | -2.18 | -1.32 | 0.68 |

**Table S9.** Gibbs free energy changes of intermediate OH adsorption ($\Delta G_{OH*}$), O adsorption ($\Delta G_{O*}$), OOH adsorption ($\Delta G_{OOH*}$), the four reaction steps ($\Delta G_1 \sim \Delta G_4$), and the overpotentials ($\eta$) of oxygen evolution reaction (OER) and oxygen reduction reaction (ORR) on $MN_4$ (M = Be, Mg, Co, Rh, Ir, Pt) monolayers with 100% M atoms participating in reaction. The results of OER and ORR are presented in red and blue color, respectively.

| System | $\Delta G_{OH*}$ (eV) | $\Delta G_{O*}$ (eV) | $\Delta G_{OOH*}$ (eV) | $\Delta G_1$ (eV) | $\Delta G_2$ (eV) | $\Delta G_3$ (eV) | $\Delta G_4$ (eV) | $\eta$ (V) |
|---|---|---|---|---|---|---|---|---|
| **$BeN_4$** | 0.39 | 3.08 | 3.61 | 0.39 | 2.69 | 0.53 | 1.31 | 1.46 |
| | | | | -1.31 | -0.53 | -2.69 | -0.39 | 0.70 |
| **$MgN_4$** | 0.26 | 2.93 | 3.53 | 0.26 | 2.67 | 0.60 | 1.39 | 1.44 |
| | | | | -1.39 | -0.60 | -2.67 | -0.26 | 0.97 |
| **$CoN_4$** | 1.11 | 2.81 | 4.07 | 1.11 | 1.70 | 1.26 | 0.85 | 0.47 |
| | | | | -0.85 | -1.26 | -1.70 | -1.11 | 0.38 |
| **$RhN_4$** | 1.40 | 3.27 | 4.21 | 1.40 | 1.87 | 0.94 | 0.71 | 0.64 |
| | | | | -0.71 | -0.94 | -1.87 | -1.40 | 0.52 |
| **$IrN_4$** | 1.32 | 2.92 | 4.25 | 1.32 | 1.60 | 1.33 | 0.67 | 0.37 |
| | | | | -0.67 | -1.33 | -1.60 | -1.32 | 0.56 |
| **$PtN_4$** | 2.05 | 4.41 | 4.54 | 2.05 | 2.37 | 0.12 | 0.38 | 1.14 |
| | | | | -0.38 | -0.12 | -2.37 | -2.05 | 1.11 |

**Table S10.** The Bader charge on metal center ($B_M$) and the adjacent four N atoms ($B_{N1}$, $B_{N2}$, $B_{N3}$, $B_{N4}$) on $MN_4$ (M = Be, Mg, Co, Rh, Ir, Pt) monolayers.

| System | $B_M$ (e) | $B_{N1}$ (e) | $B_{N2}$ (e) | $B_{N3}$ (e) | $B_{N4}$ (e) |
|---|---|---|---|---|---|
| **$BeN_4$** | 1.64 | -0.43 | -0.40 | -0.42 | -0.39 |
| **$MgN_4$** | 1.62 | -0.40 | -0.41 | -0.39 | -0.42 |
| **$CoN_4$** | 0.84 | -0.20 | -0.23 | -0.19 | -0.22 |
| **$RhN_4$** | 0.66 | -0.14 | -0.16 | -0.20 | -0.16 |
| **$IrN_4$** | 0.79 | -0.17 | -0.19 | -0.20 | -0.23 |
| **$PtN_4$** | 0.78 | -0.17 | -0.19 | -0.19 | -0.23 |